

Scheme 2.

References and Notes

- G. Ciamician, *Science* **36**, 385 (1912).
- M. Grätzel, Ed., *Energy Resources Through Photochemistry and Catalysis* (Academic Press, New York, 1983).
- M. A. Fox, M. Chanon, Eds., *Photoinduced Electron Transfer* (Elsevier, Amsterdam, 1988), parts A to D.
- J. R. Norris Jr., D. Meisel, Eds., *Photochemical Energy Conversion* (Elsevier, New York, 1989).
- N. Sutin, C. Creutz, E. Fujita, *Comm. Inorg. Chem.* **19**, 67 (1997).
- A. Hagfeldt, M. Grätzel, *Acc. Chem. Res.* **33**, 269 (2000).
- M. Grätzel, J.-E. Moser, in *Electron Transfer in Chemistry*, V. Balzani, Ed. (Wiley-VCH, Weinheim, Germany, 2001), vol. 5, part 3, chap. 1, pp. 589–644.
- G. M. Brown, B. S. Brunschwig, C. Creutz, J. F. Endicott, N. Sutin, *J. Am. Chem. Soc.* **101**, 1298 (1979).
- L. J. Heidt, A. F. McMillan, *J. Am. Chem. Soc.* **76**, 2135 (1954).
- E. Collinson, F. S. Dainton, M. A. Malati, *Trans. Faraday Soc.* **55**, 2096 (1959).
- L. J. Heidt, M. G. Mullin, W. B. Martin, A. J. M. Beatty, *J. Phys. Chem.* **66**, 336 (1962).
- K. R. Mann *et al.*, *J. Am. Chem. Soc.* **99**, 5525 (1977).
- H. B. Gray, A. W. Maverick, *Science* **214**, 1201 (1981).
- A. F. Heyduk, A. M. Macintosh, D. G. Nocera, *J. Am. Chem. Soc.* **121**, 5023 (1999).
- A. L. Odom, A. F. Heyduk, D. G. Nocera, *Inorg. Chim. Acta* **297**, 330 (2000).
- In a N_2 -filled glove box, $\text{Rh}_2^{0,II}(\text{dfpma})_3\text{Cl}_2(\text{CO})$ (185 mg, 0.230 mmol) was dissolved in 8 ml of THF and treated successively with cobaltocene (91 mg, 0.48 mmol) and triphenylphosphine (63 mg, 0.24 mmol). The solution turned red, with concomitant precipitation of yellow $[\text{CoCp}_2]\text{Cl}$. The mixture was filtered and the solvent removed in vacuo. The residue was redissolved in CH_2Cl_2 and filtered through a plug of Florisil. The volume was reduced to 5 ml and pentane was added. Cooling to -80°C overnight afforded the product as a yellow-orange microcrystalline solid (189 mg, 83% yield), which was characterized by satisfactory elemental analysis and by nuclear magnetic resonance (NMR) spectroscopy. ^1H NMR (CDCl_3) δ /ppm: 2.74 (s, 9H), 7.36 (m, 15H). ^{19}F NMR (CDCl_3) δ /ppm: -41.75 (d, $^1J_{\text{PF}}$ + $^3J_{\text{PF}}$ = 1125 Hz), -43.56 (d, $^1J_{\text{PF}}$ + $^3J_{\text{PF}}$ = 1115 Hz).
- Small-scale photolysis experiments were carried out in high-vacuum cells comprising a 1-cm clear-fused-quartz cuvette and a 20-ml solvent reservoir isolated from each other and the atmosphere by Teflon valves. Spectroscopic grade solvent was dried and added to the cell by vacuum transfer. Hydrogen halide gases (HCl from the reaction of NaCl with H_2SO_4 and HBr from a lecture bottle) were freeze-pump thawed once before transfer into the cell. Irradiation was carried out on samples maintained at 15° to 20°C with the output of a 1-kW Hg/Xe lamp. The excitation light was passed through a distilled water filter (to remove infrared light) and appropriate neutral density and colored glass filters.

- Large-scale photolysis experiments were performed in 100-ml custom high-vacuum quartz reaction tubes with a path length of ~ 2.5 cm. Sample preparation and irradiation are as in (17). After irradiation, the reaction solution was frozen, and noncondensable gas was passed through three U-traps maintained at 90 K and collected with a Toepler pump. The noncondensable gas was then combusted over hot CuO to confirm H_2 content.
- Control experiments showed no production of H_2 , as determined by Toepler pump gas collection. Irradiation of a 50-ml solution of 0.1 M HX ($\text{X} = \text{Cl}, \text{Br}$) in THF with light ($\lambda \geq 338$ nm) for 12 hours gave only an insignificant quantity of noncondensable gas

($\leq 2 \times 10^{-6}$ mol), which did not burn over CuO. Similarly, no H_2 was collected from solutions of $\text{Rh}_2^{0,II}(\text{dfpma})_3(\text{PPh}_3)(\text{CO})$ in THF containing 0.1 M HX maintained at 20°C in the dark for 12 hours.

- I. S. Sigal, K. R. Mann, H. B. Gray, *J. Am. Chem. Soc.* **102**, 7252 (1980).
- S.-S. Chern, G.-H. Lee, S.-M. Peng, *Chem. Commun.* **1994**, 1645 (1994).
- K. R. Mann, M. J. DiPierro, T. P. Gill, *J. Am. Chem. Soc.* **102**, 3965 (1980).
- A. L. Balch, M. M. Olmstead, *J. Am. Chem. Soc.* **101**, 3128 (1979).
- Solutions of $\text{Rh}_2^{0,II}(\text{dfpma})_3\text{Cl}_2(\text{PPh}_3)$ in THF containing 0.1 M HCl maintained in the dark at 20°C do not produce hydrogen as determined by Toepler pump collection of noncondensable gases. Moreover, isotopic scrambling involving the solvent is not observed. Photolysis of $\text{Rh}_2^{0,II}(\text{dfpma})_3\text{Cl}_2(\text{PPh}_3)$ in d^8 -THF containing 10 equiv of HCl results in the exclusive production of H_2 over the first 3 hours of irradiation, as evidenced by the appearance of a singlet in the ^1H NMR at 4.53 ppm (H_2). Continued irradiation gives subsequent formation of HD ($\delta = 4.50$ ppm, $^1J_{\text{HD}} = 43$ Hz), as expected from halogen trapping by d^8 -THF to generate DCl. The deuterated acid then enters the photocatalytic cycle to produce HD and D_2 .
- C. Woodcock, R. Eisenberg, *Inorg. Chem.* **23**, 4207 (1984).
- D. Evans, G. Yagupsky, G. Wilkinson, *J. Chem. Soc. A* **1968**, 2660(1968).
- T. A. Albright, J. K. Burdett, M.-H. Whangbo, *Orbital Interactions in Chemistry* (Wiley-Interscience, New York, 1985).
- Supported by a grant from the NSF (grant CHE-9817851).

30 May 2001; accepted 23 July 2001

Design of Bioelectronic Interfaces by Exploiting Hinge-Bending Motions in Proteins

David E. Benson,^{1*} David W. Conrad,¹ Robert M. de Lorimier,¹ Scott A. Trammell,² Homme W. Hellinga^{1†}

We report a flexible strategy for transducing ligand-binding events into electrochemical responses for a wide variety of proteins. The method exploits ligand-mediated hinge-bending motions, intrinsic to the bacterial periplasmic binding protein superfamily, to establish allosterically controlled interactions between electrode surfaces and redox-active, Ru(II)-labeled proteins. This approach allows the development of protein-based bioelectronic interfaces that respond to a diverse set of analytes. Families of these interfaces can be generated either by exploiting natural binding diversity within the superfamily or by reengineering the specificity of individual proteins. These proteins may have numerous medical, environmental, and defense applications.

Hybrid devices consisting of biological and abiotic components combine the exquisite molecular recognition properties and complex activities of biomolecules with the power of existing electrochemical (1–6), optical (7–12), magnetic (13, 14), or mechanical (15) technologies. Central to the development of such devices is the con-

struction of interfaces that transduce biomolecular events such as ligand binding into abiotic signals (6, 16) or actions (17, 18). Ideally, it should be possible to build families of biomolecular interfaces that respond to a wide variety of chemical stimuli (19). A biomolecular interface comprises three different functions: molecular recog-

nitiation and signal transduction within the biomolecules, and detection of the signal by the abiotic component. The major obstacle to developing families of interfaces is the difficulty in identifying biomolecules in which these three functions are sufficiently independent to attain a high diversity in molecular recognition while keeping signal transduction and detection mechanisms constant. Ligand-mediated macromolecular structural changes have been used to link molecular recognition and signal transduction while keeping the sites for these two functions sterically separated (19). Examples include reversible assembly reactions of proteins (1, 4, 5, 12, 13, 18) or nucleic acids (2, 14, 15), gating of transmembrane pores (3), and macromolecular conformational changes (10, 11). However, allosteric interactions in proteins, one of the main structural mechanisms by which biological systems establish linkage between disparate activities (20), has not yet been widely explored (7–9). Here, we demonstrate how protein allosteric interactions can be designed to transduce ligand binding into

electrochemical signals, and show that this leads to a strategy for building families of chemoresponsive bioelectronic interfaces.

In many proteins, two sites are thermodynamically coupled (allosterically linked) when each site adopts multiple local conformations that correspond to distinct global protein conformations (20). Global conformational changes that establish allosteric linkage often correspond to different quaternary states in multimeric assemblies (21), but may also involve motions such as ligand-induced hinge-bending motions (21) within monomers. Such motions are found in many proteins (21), and are common to all structurally characterized members of the bacterial periplasmic binding protein (bPBP) superfamily. Here, we show that it is possible to couple ligand binding in bPBPs to modulation of the interactions between a redox reporter group and a modified electrode surface.

Maltose-binding protein (MBP) is a structurally well-characterized member of the bPBP family (22). This protein adopts two conformations: a ligand-free open form and a liganded closed form, which interconvert by a hinge-bending motion (Fig. 1). To couple ligand binding to an electrochemical response, we designed a conformational coupling mechanism to modulate the behavior of a redox reporter group. The COOH-terminus (near the hinge-region) of MBP was tethered to the electrode, and a Ru(II) redox reporter group was conjugated

site-specifically to a mutant cysteine designed to be placed on the surface of MBP that faces the electrode (Fig. 1). This arrangement is designed to orient the ligand-binding site toward the bulk solution, and link the ligand-mediated conformational changes within the MBP-electrode interface to alterations in electronic coupling between the Ru(II) reporter group and the electrode, thereby allowing ligand binding to be measured electrochemically.

The presence of an electroactive protein layer consisting of MBP labeled with the Ru(II) cofactor at position Gly174Cys on a surface-modified electrode (23) was confirmed by measuring cyclic voltammograms (24). At fast scan rates (4 V/s), robust, cyclic voltammograms with small peak separations (~30 mV) were observed, indicative of a surface immobilized redox cofactor (25) (Fig. 2). This signal was not observed in electrodes modified with unlabeled MBP. The midpoint potential of the MBP-Ru(II) conjugate (+220 mV) is consistent with immobilization, because it is similar to the measured potential of the Ru(II) reporter directly tethered to a modified gold electrode (+240 mV) (24), and not to that observed in the MBP-Ru(II) conjugate in solution (+330 mV) (26). The current observed in the cyclic voltammogram is consistent with 10 to 30% coverage of the electrode surface by redox-active immobilized MBP-Ru(II) conjugates (24), indicating that the formation of protein multilayers is unlikely. The electrochemical signal due to the Ru(II) reporter group vanished when any one of the three tethering components [His-tag, Ni(II), nitrilotriacetate groups, see caption of Fig. 1] was omitted. Addition of a competing ligand, imidazole, also resulted in complete loss of

¹Department of Biochemistry, Box 3711, Duke University Medical Center, Durham, NC 27710, USA.
²Center for Biomolecular Science and Engineering, Code 6900, Naval Research Laboratory, Washington, DC 20375, USA.

*Present address: Wayne State University, Department of Chemistry, Detroit, MI 48202, USA.
 †To whom correspondence should be addressed. E-mail: hwh@biochem.duke.edu

Fig. 1. (A) Ligand-induced protein conformational changes in ruthenium-labeled maltose binding protein (MBP). The attachment site of the synthetic Ru(II) redox cofactor is indicated by the large gray sphere; the COOH-terminus by the labeled white sphere. All molecular graphics were generated with Molscrip (37). **(B)** Schematic illustration of the protein-mediated, ligand-dependent changes in the interaction between the Ru(II) redox reporter group and the surface-modified gold electrode. Proteins were attached to the electrode by modifying the gold surface with a self-assembled monolayer of hydroxyl- and Ni(II)-nitrilotriacetate-terminated headgroups (24) to which the protein was site-specifically coordinated through a COOH-terminal oligohistidine (rectangle). The thiol-reactive ruthenium complex (ball) was covalently linked to a mutant cysteine on the protein surface, thereby positioning the metal complex at the interface between the protein and self-assembled monolayer. Upon ligand binding (square), the changes in the protein conformation [open (left) → closed (right)] alter the interaction between the cofactor and electrode surface, and hence the observed current flowing between these two components.

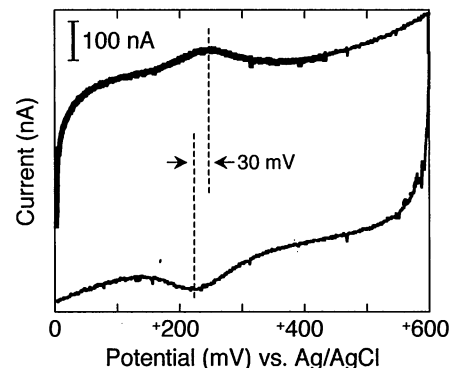
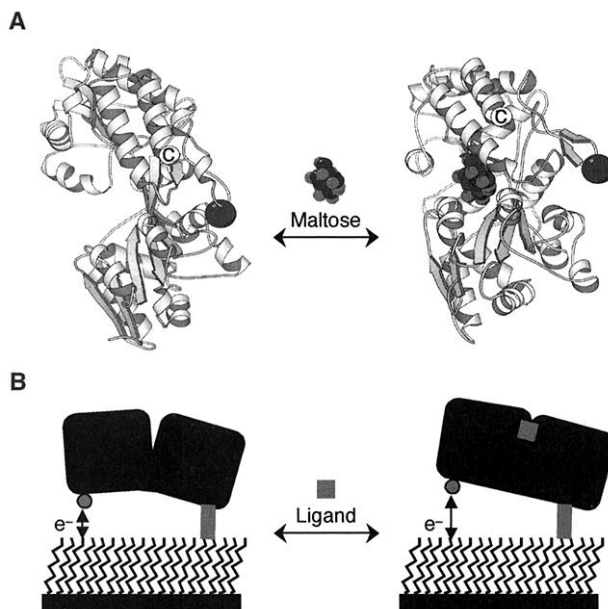


Fig. 2. Cyclic voltammogram of a Ru(II)-labeled G174C MBP mutant immobilized on a surface-modified gold electrode (24). The measurements were taken at a scan rate of 4 V/s. The observed 30 mV peak separation is indicative of surface immobilized redox-active species (25). Integration of the peak currents revealed that 10 to 30% of the electrode surface is covered with electroactive protein.

REPORTS

signal. Addition of 3 M guanidinium HCl followed by dilution of this protein denaturant reversibly eliminated and restored the signal. These observations are consistent with formation of an electroactive layer consisting of a folded, electrochemically active protein conjugate, tethered to the modified electrode.

The ligand dependence of the electrochemical response was probed using ac voltammetry (25, 27). The optimal ac current response (28) due to the Ru(II) reporter group was observed at 1 kHz (24), and decreased from 12 to 4 μ A upon addition of maltose (Fig. 3A). The ligand concentration dependence of the ac current fit to a single-site binding isotherm (Fig. 3A), and only the addition of maltose (and not glucose, glutamine, or zinc) elicited an electrochemical response. Additional modified electrodes were prepared using MBP point

mutants with decreased affinities for maltose (7). The observed maltose affinities of the resulting modified electrodes varied according to the solution binding constants of the mutant proteins (Fig. 4). All the electrochemically determined affinities correlate within a factor of four to those measured for the proteins free in solution (29). These observations are all consistent with a specific, ligand-mediated electrochemical response of the protein-modified electrode.

To demonstrate the generality of the use of the hinge-bending mechanism, we constructed additional chemoresponsive electrodes using two other members of the bBPB superfamily: glucose-binding protein (GBP) (30) and glutamine-binding protein (QBP) (31). MBP, QBP, and GBP have similar overall structures but little sequence homology (32). Even so, the GBP- and QBP-modified electrodes exhibited similar

ac currents (0.5 to 10 μ A), midpoint potentials (+220 to 230 mV), optimal frequencies (0.1 to 1 kHz), and ligand-mediated ac current changes (Fig. 3, B and D) as the MBP-modified electrodes. The currents decreased in response to addition of cognate ligand only (33), with affinities similar to those observed for protein free in solution (29).

Finally, we constructed a protein-modified electrode using an MBP redesigned to bind Zn(II) (eZBP) (9) to demonstrate that new sensors can be developed in a modular fashion by re-engineering the ligand-binding site without destroying the linkage to the reporter group (19). The electrochemical response of the eZBP-modified electrode (Fig. 3C) was identical to wild-type MBP, but changed in response to zinc, rather than maltose (29, 33).

To demonstrate that the engineered sensors measure analyte concentrations in complex, "real" samples, we constructed a titration curve of glucose with GBP in rat serum, and of maltose with MBP in beer. The glucose measurements were taken using glucose-depleted rat serum, and adding back known concentrations of glucose-fortified serum. The resulting glucose-binding curve ($K_d = 4.1 \mu$ M) was nearly identical to the one obtained in a simple buffer ($K_d = 4.0 \mu$ M). The concentration of maltose in beer is relatively high (~0.1 to 0.2 M), and we therefore used the MBP W340A mutant, which has a K_d that is appropriate for measuring these concentrations. The electrochemically determined maltose concentration in the brand of beer we used was found to be 102 mM (3.69 g/100 ml). This measurement correlates to within 5% error with concentrations determined independently

Fig. 3. Ligand-mediated responses of allosterically controlled electrochemical assemblies derived from a family of engineered periplasmic binding proteins. (A) Maltose sensor using a G174C mutant of MBP [1 kHz; $^{\circ}K_d$ (maltose) = 4 μ M; fK_d (maltose) = 1 μ M]. (B) Glucose sensor using a Leu255Cys mutant of GBP [0.1 kHz; $^{\circ}K_d$ (glucose) = 2.0 μ M; fK_d (glucose) = 0.4 μ M]. (C) Zinc sensor using a redesigned variant of G174C-MBP [1 kHz; $^{\circ}K_d$ (zinc) = 10 μ M; fK_d (zinc) = 3 μ M]. (D) Glutamine sensor using an Glu163Cys mutant of QBP [0.16 kHz; $^{\circ}K_d$ (glutamine) = 1.0 μ M; fK_d (glutamine) = 0.2 μ M]. Two binding constants are reported: $^{\circ}K_d$ is dissociation constant of the assembly, determined electrochemically; fK_d is the dissociation constant of the protein free in solution, determined by measuring changes in the intrinsic tryptophan fluorescence of the conjugates (29). Fractional saturation curves (left graphs) were constructed by fitting the baseline-corrected ac currents (right graphs) measured at different ligand concentrations to a standard binding isotherm (7). The binding curves represent the average of at least three determinations, with error bars smaller than the plot symbols.

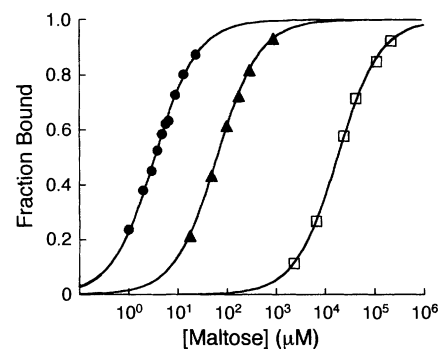
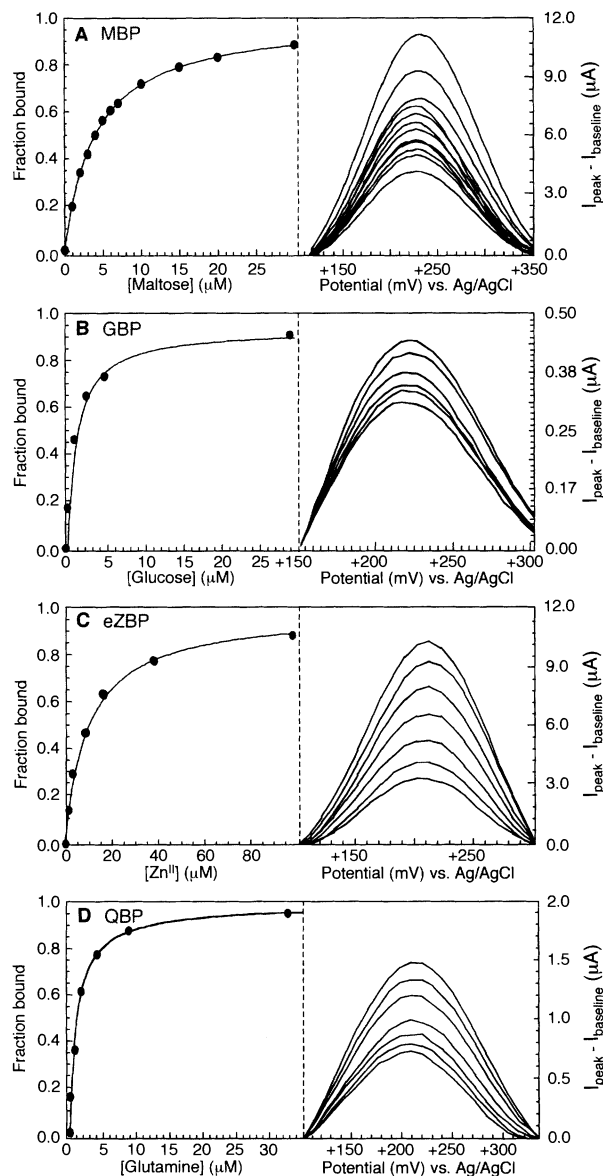


Fig. 4. Effect of mutations in the binding pocket of MBP on maltose-dependent electrochemical responses. Ligand-dependent peak currents (average of at least three determinations; error bars are smaller than the symbol) were fitted to a binding isotherm (7). Filled circles, L174C-MBP ($^{\circ}K_d = 4 \mu$ M; $^fK_d = 1 \mu$ M); filled triangles, Trp62Ala L174C-MBP ($^{\circ}K_d = 62 \mu$ M; $^fK_d = 15 \mu$ M); open squares, Trp340Ala L174C-MBP ($^{\circ}K_d = 18 \mu$ M; $^fK_d = 3 \mu$ M).

REPORTS

by enzymatic assay (Fig. 5). These experiments show that the behavior of the modified electrodes is not adversely affected by different sample matrices that contain a multitude of potential interferents such as proteins (serum) and small molecules (beer), demonstrating their potential to function as sensors in complex mixtures.

The majority of protein-based electrochemical biosensors developed to date are based on detecting enzymatic activity (34), whereas the allosterically controlled electrochemical (ACE) assemblies presented here are nonenzymatic. In enzyme-based systems, each signal transduction mechanism has to be tailor-made to the analyte, whereas the signal transduction mechanism is the same in each ACE assembly. In a nonenzymatic biosensor, no additional reagents have to be supplied, nor does detection depend on diffusible products. Nonenzymatic detection potentially simplifies the development of new sensors by the engineering of binding specificity, because no catalytic mechanisms have to be maintained, as we have clearly demonstrated by the radical change of a maltose sensor into a zinc sensor that retains signal transduction. The detection range of nonenzymatic sensors is dictated by the ligand-binding constants, and allows detectors for different dynamic ranges to be built by manipulating the affinity (Fig. 4), the advantage of which we have demonstrated by measuring an analyte present at high concentrations. The lower limit of detection is determined in large part by the tightest binding constant that can be obtained, which is ~ 1 nM for this class of protein (32), and appropriate

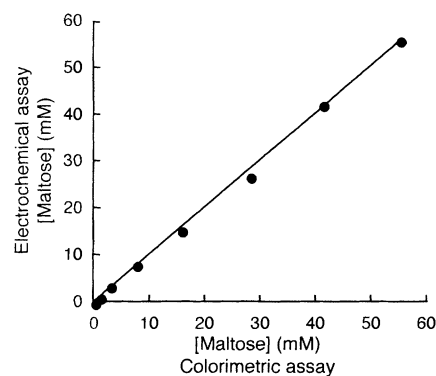


Fig. 5. Correlation of enzymatic (40) and electrochemical maltose assays in beer using W340A L174C-MBP. The electrochemical assay was performed by first constructing a standard binding curve with maltose titrated into buffer. Second, beer was titrated into buffer (0 to 70% v/v), and the relationship between added volume and fractional electrochemical response was obtained. The fractional electrochemical response was then used to determine the corresponding maltose concentration from the standard curve.

for many clinical applications (35).

The only other nonenzymatic electrochemical protein sensors developed so far are based on detecting the flow of ions across a membrane through transmembrane pores that are gated by ligand binding (1, 3). In one such system, binding of antigen to antibodies is coupled to the assembly of an open gramicidin channel (1). In another, flow of ions through α -hemolysin is controlled either by making ligand-binding mutations in the channel, or by inserting clathrands into the channel (3). These systems require the construction of complex, multicomponent macromolecular assemblies, whereas the ACE assemblies are relatively simple.

The success obtained with the different proteins presented in this work demonstrates that construction of allosterically controlled electroactive assemblies is a generalizable strategy for developing families of chemoresponsive biomolecular interfaces. Sensors for different analytes can be developed either by exploiting the natural diversity provided by the wide variety of proteins that undergo ligand-mediated hinge-bending motions (21), or by engineering ligand-binding specificities using a combination of computational and directed evolution approaches (36). Even within the limited exploration of receptors presented here, we have developed sensors that have application in fermentation technology (maltose, glutamine), and clinical chemistry (glucose, zinc). This approach therefore represents a first step toward the development of large families of bioelectronic sensors capable of precisely and accurately sensing a diverse set of analytes that may have numerous medical, environmental, and defense applications (4, 16, 17, 19).

References and Notes

1. B. A. Cornell *et al.*, *Nature* **387**, 580 (1997).
2. E. M. Boon, D. M. Ceres, T. G. Drummond, M. G. Hill, J. K. Barton, *Nature Biotechnol.* **18**, 1096 (2000).
3. L.-Q. Gu, S. Cheley, H. Bayley, *Science* **291**, 636 (2001).
4. I. Willner, E. Katz, *Angew. Chem. Int. Ed.* **39**, 1180 (2000).
5. S. Schutz *et al.*, *Sens. Actuators B* **65**, 291 (2000).
6. W. Göpel, *Sens. Actuators B* **52**, 125 (1998).
7. J. S. Marvin *et al.*, *Proc. Natl. Acad. Sci. U.S.A.* **94**, 4366 (1997).
8. J. S. Marvin, H. W. Hellinga, *J. Am. Chem. Soc.* **120**, 7 (1998).
9. _____, *Proc. Natl. Acad. Sci. U.S.A.* **98**, 4955 (2001).
10. Q. Cheng, R. C. Stevens, *Adv. Mater.* **9**, 481 (1997).
11. Y. Shen, C. R. Safinya, K. S. Liang, A. F. Ruppert, K. J. Rothschild, *Nature* **366**, 48 (1993).
12. Y. Tang, B. C. Dave, *Adv. Mater.* **10**, 1536 (1998).
13. Y. R. Chelma *et al.*, *Proc. Natl. Acad. Sci. U.S.A.* **97**, 14268 (2000).
14. R. L. Edlestein *et al.*, *Biosens. Bioelectron.* **14**, 805 (2000).
15. J. Fritz *et al.*, *Science* **288**, 316 (2000).
16. J. M. Laval, P. E. Mazeran, D. Thomas, *Analyst* **125**, 29 (2000).
17. C. R. Lowe, *Curr. Opin. Chem. Biol.* **10**, 428 (2000).
18. R. K. Soong *et al.*, *Science* **290**, 1555 (2000).

19. H. W. Hellinga, J. S. Marvin, *Trends Biotechnol.* **16**, 183 (1998).
20. M. Perutz, *Mechanisms of Cooperativity and Allosteric Regulation in Proteins* (Cambridge Univ. Press, Cambridge, 1990).
21. M. Gerstein, A. M. Lesk, C. Chothia, *Biochemistry* **33**, 6739 (1994).
22. F. A. Quiocho, J. C. Spurlino, L. E. Rodseth, *Structure* **5**, 997 (1997).
23. N. H. Thomson *et al.*, *Biophys. J.* **76**, 1024 (1999).
24. Mutant proteins were constructed, purified, and derivatized as described in (7, 8). The Ru(II) reporter group, [Ru(II)(NH₃)₄(1,10-phenanthroline-5-maleimide)](PF₆)₂, was synthesized as described (26). An 11-thioundecanoic acid-derivatized gold electrode was activated with 1-(3-dimethylaminopropyl)-3-ethylcarbodiimide HCl, reacted with lysine-nitrilotriacetate (NTA) and 5-aminopentanol (1:20 ratio), and charged with Ni(II), forming a Ni(II)-NTA and OH-terminated monolayer (23). See supplementary information (www.sciencemag.org/cgi/content/full/293/5535/1641/DC1) for detailed descriptions of preparation of the modified electrode, protein immobilization, electrochemical methods, determination of electroactive protein surface coverage, and reduction potential of Ru(II) reporter group directly tethered to the surface-modified gold electrode.
25. A. J. Bard, L. R. Faulkner, *Electrochemical Methods* (Wiley, New York, 1980).
26. S. A. Trammell, L. M. Tender, D. W. Conrad, D. E. Benson, H. W. Hellinga, *Bioconjug. Chem.* **12**, 643 (2001).
27. S. E. Creager, T. T. Wooster, *Anal. Chem.* **70**, 4257 (1998).
28. The optimal frequency for ac voltammograms was determined using a ratio of ac peak current to baseline current (27). This method is used to partially correct for capacitive contributions to the total observed current, thereby providing a relatively specific probe for the Faradaic contributions by the Ru(II) reporter group. The baseline current was linearly interpolated between the extrema of the potentiometric peak (24). In the single frequency potential scans currents are reported as a difference between the ac peak and baseline currents, since there is no need for frequency correction of current response.
29. For every protein presented in this study, the ligand-binding affinities determined electrochemically using a gold disk electrode are two to five times weaker than those in solution. However, if a gold microelectrode prepared by flame annealing a gold wire (27) is used instead of a gold disk electrode, the electrochemically determined affinities are similar to the solution affinities. This indicates that the atomic structure of the gold electrode surface is an important contributor to the interactions between the electrode and the protein.
30. N. K. Vyas, M. N. Vyas, F. A. Quiocho, *Science* **242**, 1290 (1988).
31. C. D. Hsiao, Y. J. Sun, J. Rose, B. C. Wang, *J. Mol. Biol.* **262**, 225 (1996).
32. R. Tam, M. H. Saier, *Microbiol. Rev.* **57**, 320 (1993).
33. All proteins were tested with the following ligands: maltose, glucose, glutamine, glutamate, and zinc. In all cases, only addition of the cognate ligand elicited an electrochemical response.
34. A. E. G. Cass, Ed., *Biosensors: A Practical Approach* (Oxford Univ. Press, Oxford, 1990).
35. C. A. Burtis, E. R. Ashwood, Eds., *Clinical Chemistry* (Saunders, Philadelphia, PA, 1994).
36. F. H. Arnold, *Nature* **409**, 253 (2001).
37. P. J. Kraulis, *J. Appl. Crystallogr.* **24**, 946 (1991).
38. Maltose/Sucrose/D-glucose colorimetric assay kit (R-Biopharm).
39. We thank A. E. G. Cass for initial help, C. D. Paavola for providing the plasmid for glutamine binding protein, and M. S. Wisz for help in reviewing the manuscript. This work was supported by an NIH grant (H.W.H.), an Office of Naval Research grant (H.W.H., D.W.C., and R.M.L.), an NIH postdoctoral fellowship (D.E.B.), and a National Research Council postdoctoral fellowship (S.A.T.).

11 May 2001; accepted 24 July 2001